Electronic Supplementary Material (ESI) for ChemComm.

Supporting Information for

Autonomous optimisation of a nanoparticle catalysed reduction reaction using a continuous flow reactor system

Brendan L. Hall, Connor J. Taylor, Ricardo Labes, Alexander F. Massey, Robert Menzel, Richard A. Bourne and Thomas W. Chamberlain*

Institute for Process Research and Development, School of Chemistry, University of Leeds, Leeds, LS2 9JT, UK. E-mail: T.W.Chamberlain@Leeds.ac.uk; Fax: +44 (0)113 432215

Table of Contents

1 Reservoir preparation, chemicals and reaction conditions

1.1 List of chemicals and suppliers

Chloroauric Acid: Supplier: Fisher Chemical, CAS: 16903-35-8, Cat no: 10765131, Melting Point: 30 °C, Molecular Formula: $HAuCl_4$, Packaging: Vial, Quantity: 1 g, Formula Weight: 339.78 g/mol, MDL Number: 149903, Physical Form: Orange Solid.

Sodium citrate tribasic dihydrate. Supplier: Merck Life Science UK Limited, Manufacturer: Sigma Aldrich, CAS Number 6132-04-3, Cat no :71402-100G, Manufacturer part number:71402 Description: Sodium citrate tribasic dihydrate, Bio Ultra, for molecular biology, >=99.5% (NT). Physical Form: White Solid.

4-Nitrophenol. Supplier: Merck Life Science UK Limited, Manufacturer: Sigma Aldrich, CAS Number 100-02-7, Cat no: 241326-50G, Manufacturer part number: 241326. Physical Form: Yellow Solid.

Sodium Borohydride. Supplier: Supplier: Merck Life Science UK Limited, Manufacturer: Sigma Aldrich, CAS: 16940-66-2, Cat no: 71320-25G, Manufacturer part number:71320. Molecular Formula $NaBH_4$, Molecular Weight 37.83. Physical Form: White Solid.

Ultra-pure water. Type 1 ultra-pure water purified to a resistivity of 18 MΩ cm^{-1} with a Purelab Flex Pure Water System was used throughout this study.

1.2 Preparation of reservoir solutions

1.2.1 Nitrophenol

Nitrophenol (83.46 mg) was dissolved in 1000 mL of water.

1.2.2 $NaBH_4$

To prevent hydrolysis of $NaBH_4$ during the course of the optimisation the solution reservoir was prepared as follows. $NaBH_4$ was dissolved in 600 mL of ice-cold water and maintained at 0 °C by placing the beaker containing the sodium borohydride solution in an insulated ice bath and adjusted to pH 10 by dropwise addition of 0.1 M sodium hydroxide solution. The cooled $NaBH_4$ (aq) solution was passed through a heat exchange coil (0.5 m, 1/32" ID PTFE tubing), submerged in a water bath at room temperature, so the $NaBH_4$(aq) solution reached room temperature before entering the reactor.

1.2.3 Gold nanoparticle catalyst

The gold nanoparticle (AuNP) solution was synthesised using a standard Turkevich approach adapted from N.G. Bastus. [1] Chloroauric Acid (aq) (25 mM, 1 mL) was injected rapidly into a 3 necked 250 mL round bottomed flask containing a stirred solution of sodium citrate (2.2 mM, 149 mL) at 95 °C with a reflux condenser, the solution turned from pale yellow to greyish blue before turning pink then ruby red, the reaction was heated and stirred for 30 minutes then allowed to cool to room temperature.

2 AuNP catalyst characterisation

2.1 AuNP UV-vis analysis

The AuNP solution (synthesis method described in section 1.3) was added without dilution to a quartz cuvette (1 cm path-length) and placed in an OceanOptics CUV UV cuvette holder. The UV-vis spectra were obtained using a FLAME-S-US-VIS diode-array detector type spectrometer (200-850 nm) from OceanOptics with a DH-MINI deuterium tungsten halogen light source (200-2000 nm) and QP400-2-SR-BX 400 um premium fibre optic cables. The UV-vis absorption spectra shown in Figure S1 was averaged from spectra taken once a second over a period of 30 seconds.

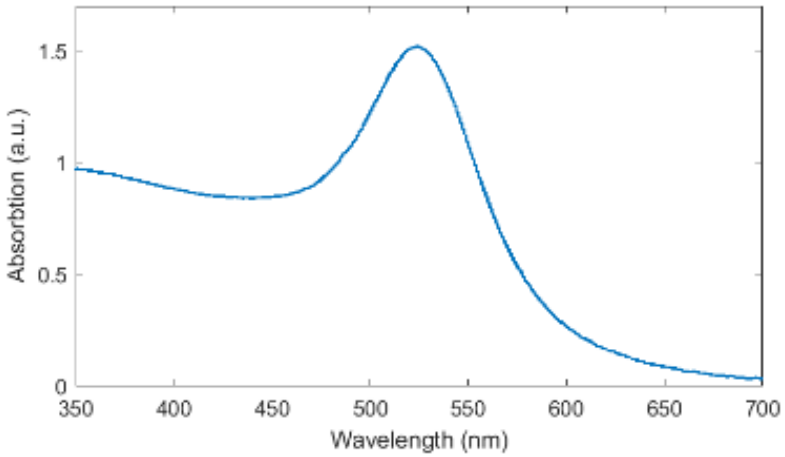

Figure S1. UV-vis spectra of the AuNP solution prepared using the method described in section 1.2.3.

2.2 Surface area

The active surface area of Au nanoparticles in the reaction (S) was calculated using a geometric approximation which assumed that all the gold nanoparticles (AuNPs) are the same size and have a 'spherical', FCC structure, see equation 1. Where r is the average AuNP radius (7.85 nm, determined by TEM analysis, see Figure S3 - section 2.4.1), C_{Au} is the concentration of Au atoms in a given reaction and a is the FCC unit cell length for bulk Au (0.407 nm), where each unit cell contains 4 atoms.[2] The number of atoms contained within each AuNP was calculated by dividing the nanoparticle volume by the unit cell volume and multiplying by 4. Dividing Avogadro's constant (N_A) by the average number of atoms contained within each AuNP gives the number of nanoparticles per mol of Au atoms, multiplying this value by the nanoparticle surface area gives a correlation constant with the units (m^2mol^{-1}). This constant can be multiplied by the concentration of Au atoms in the reaction to give S for each reaction (m^2L^{-1}).

$$S = \frac{N_A}{\left(\left(\frac{\frac{4}{3}\pi r^3}{a^3}\right)\cdot 4\right)} C_{Au} 4\,\pi\, r^2 \qquad (1)$$

2.3 AuNP DLS size distribution analysis

The AuNP solution (synthesis method described in section 1.3) was added without dilution to a 1 cm path-length plastic disposable cuvette. Dynamic light scattering (DLS) size distribution analysis was performed using a Malvern Zetasizer Nano. Sample measurements were taken at 25 °C with equilibration time of 120 seconds, 11 runs were performed per measurement each with an acquisition time of 10 seconds. DLS measurements were performed three times and the results are shown in Figure S2. For sample 1 (Figure S2) the recorded Z-average diameter was 25.74 nm with a standard deviation of 16.05 nm, (count rate of 160.7 kcps and polydispersity index 0.210).

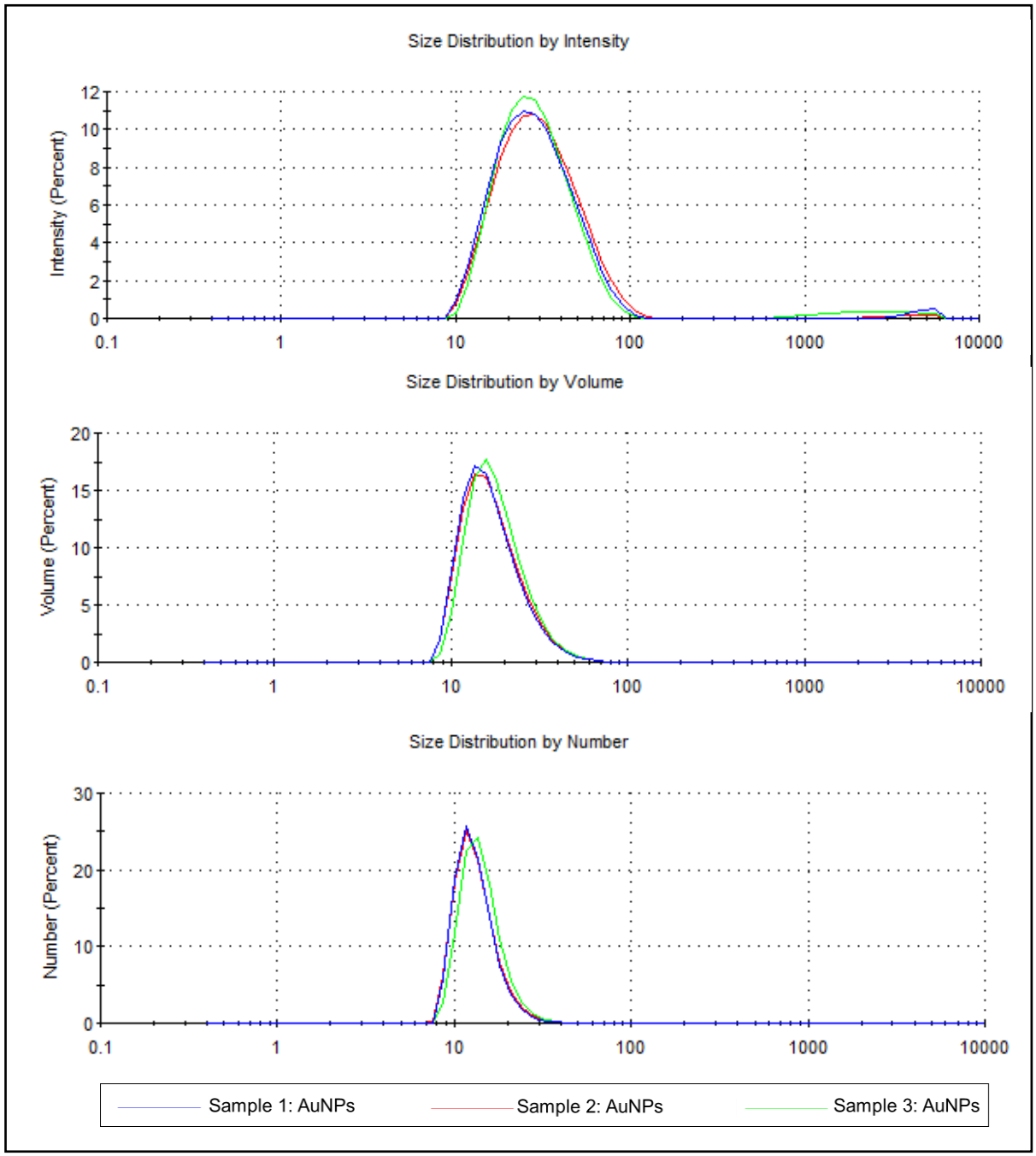

Figure S2. DLS analysis of the AuNP solution prepared using the method described in section 1.2.3, with plots showing the size distribution by intensity, volume and number percent.

2.4 Transmission electron microscopy (TEM) analysis

TEM analysis was used to characterise the AuNPs (synthesis method described in section 1.2.3), to evaluate the variation in NP size, both before and after the nanoparticles were used to catalyse a nitrophenol reduction reaction (section 6.1). Both samples were prepared for TEM by taking a solution of the AuNPs (5 drops dispersed in isopropanol (2 mL) using an ultrasonic bath) and depositing it on a holey carbon film coated copper grid.

TEM images were acquired on a FEI Tecnai TF20 field emission gun microscope operating at 200 kV. For both samples, the NP size distribution histograms were obtained from the measurements of 120 different NPs per sample assuming a spherical shape and with random distribution.

2.4.1 Particle size distributions (before/after reaction)

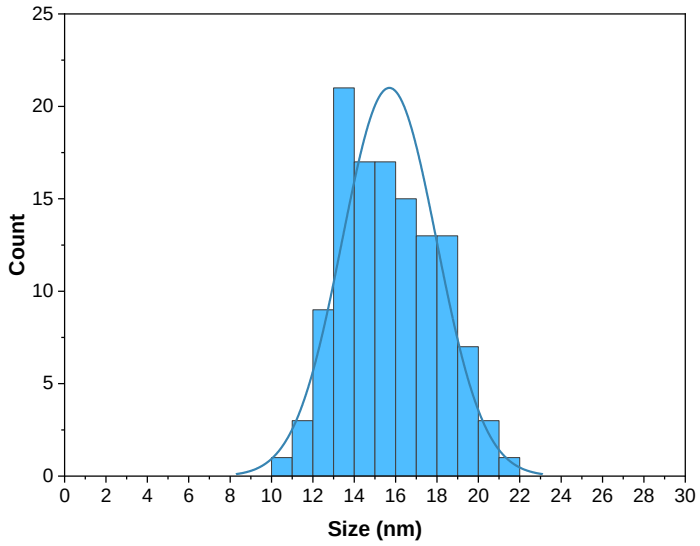

Figure S3. Size distribution histogram for 120 manually sized AuNPs taken before the nanoparticles were used to catalyse the reduction of nitrophenol (diameter: 15.7 ± 5.5 nm) from TEM micrographs shown in ESI section 2.4.2.

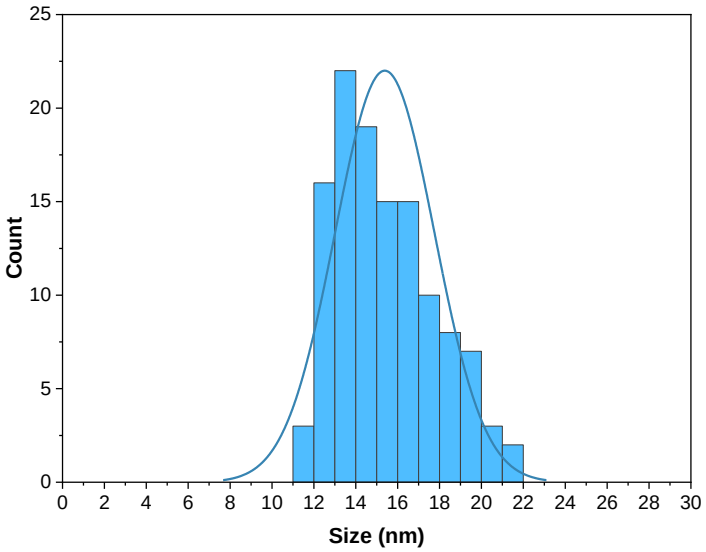

Figure S4. Size distribution histogram for 120 manually sized AuNPs taken after the nanoparticles were used to catalyse the reduction of nitrophenol (diameter: 15.4 ± 5.9 nm) from TEM micrographs shown in ESI section 2.4.3.

2.4.2 TEM images - particle size distribution (before reaction)

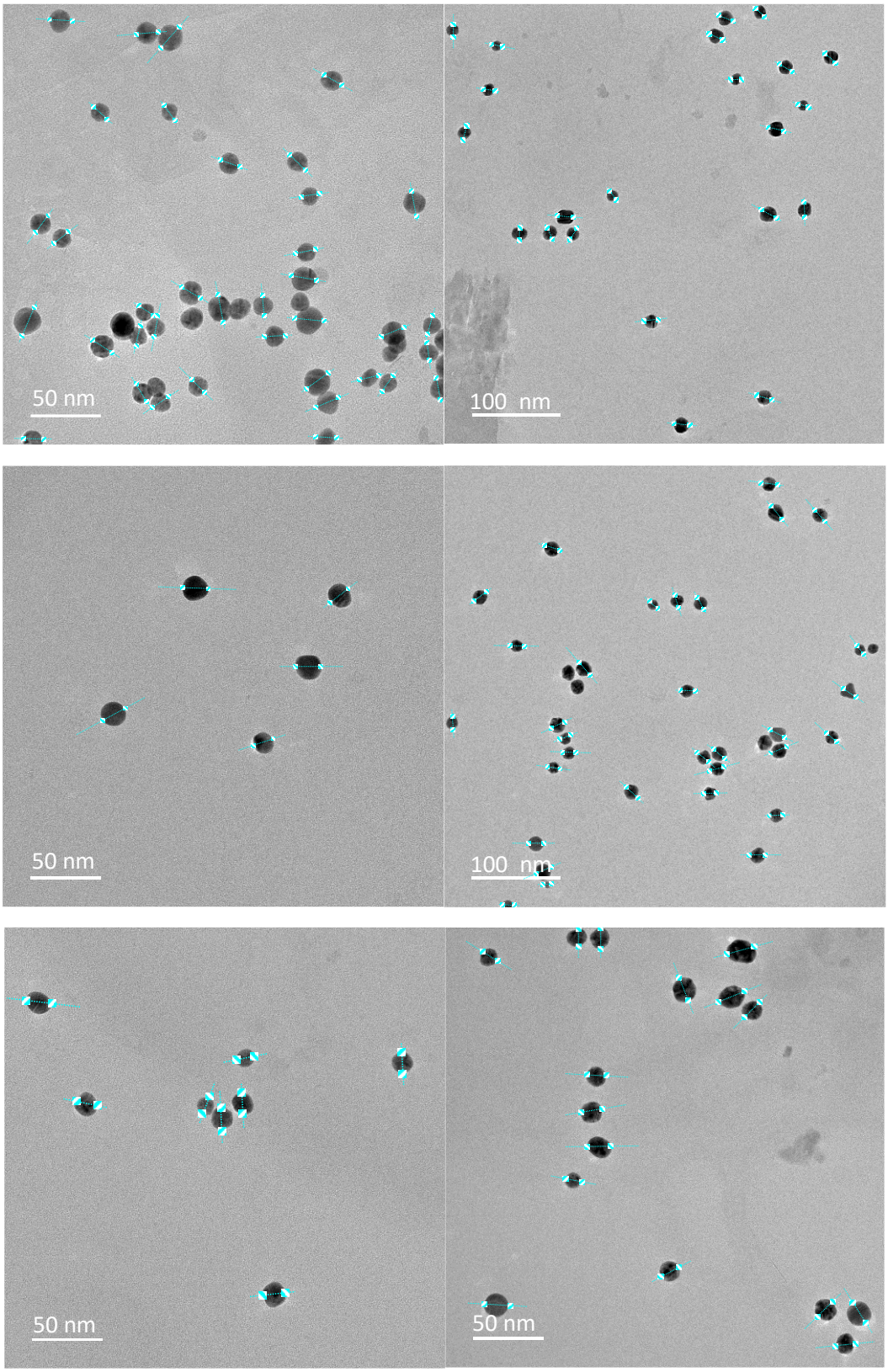

Figure S5. TEM images used to obtain the size distribution histogram shown Figure S3 (before reaction).

2.4.3 TEM images - particle size distribution (after reaction)

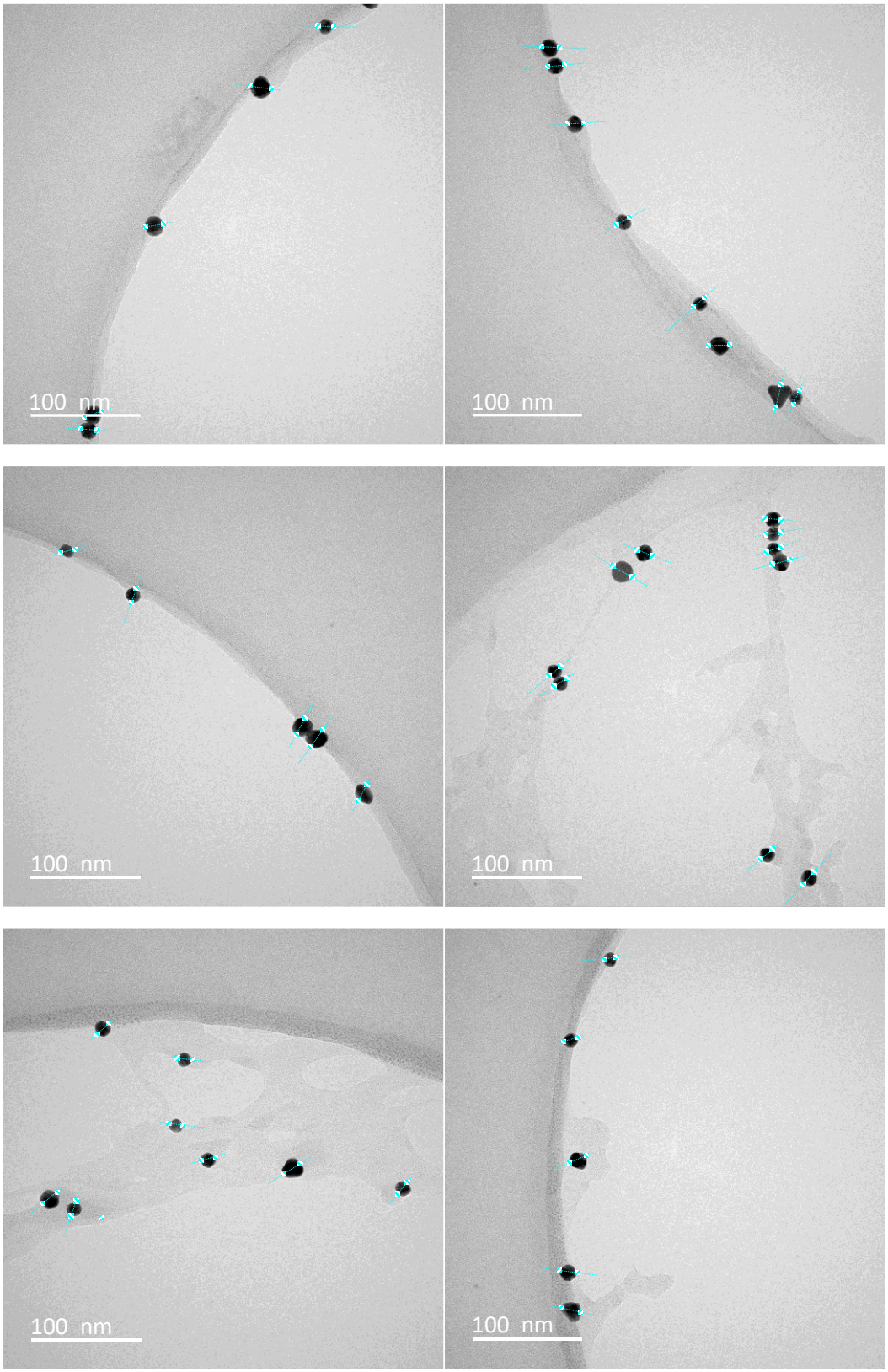

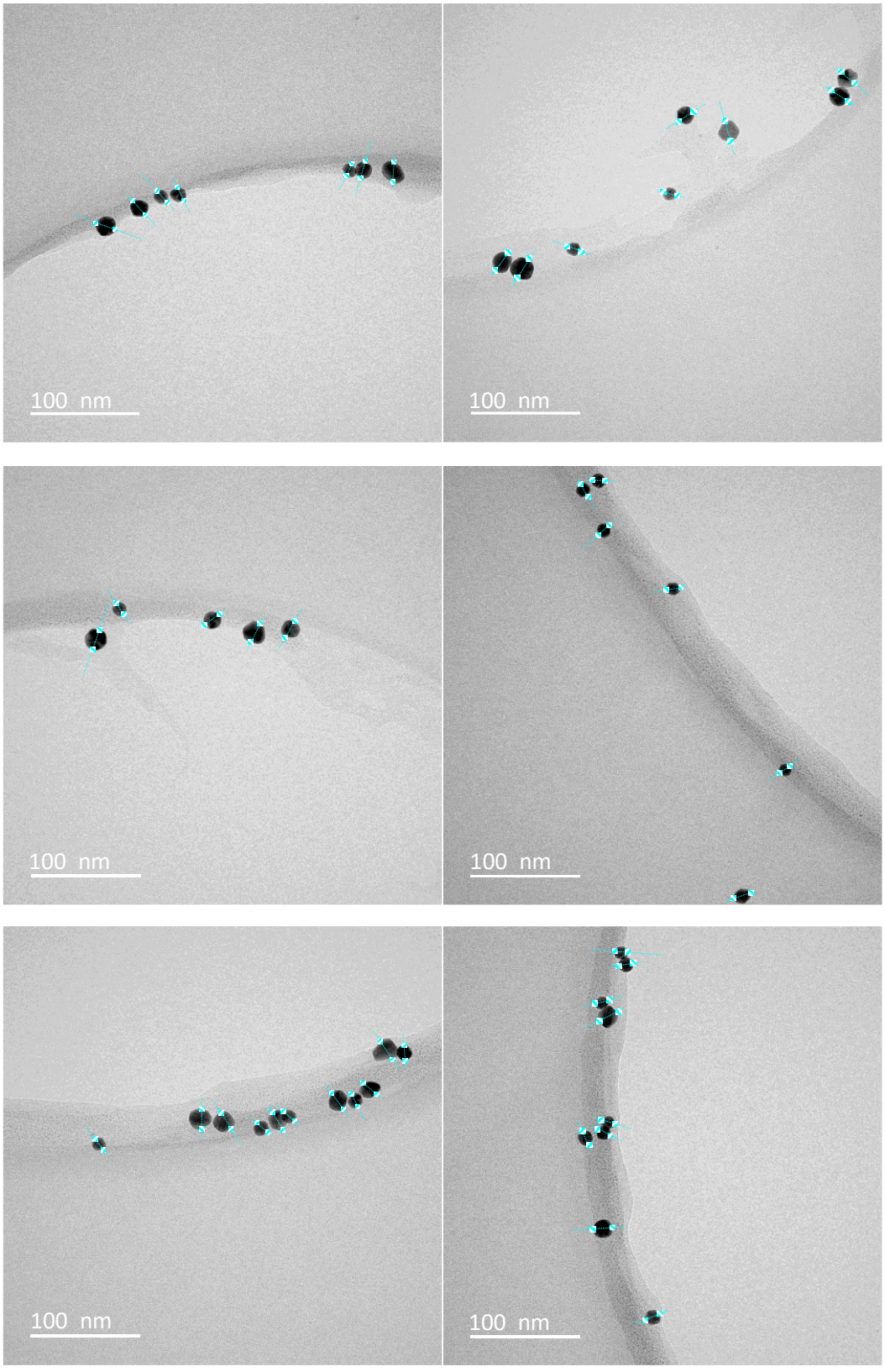
100 nm
100 nm
100 nm
100 nm
100 nm
100 nm

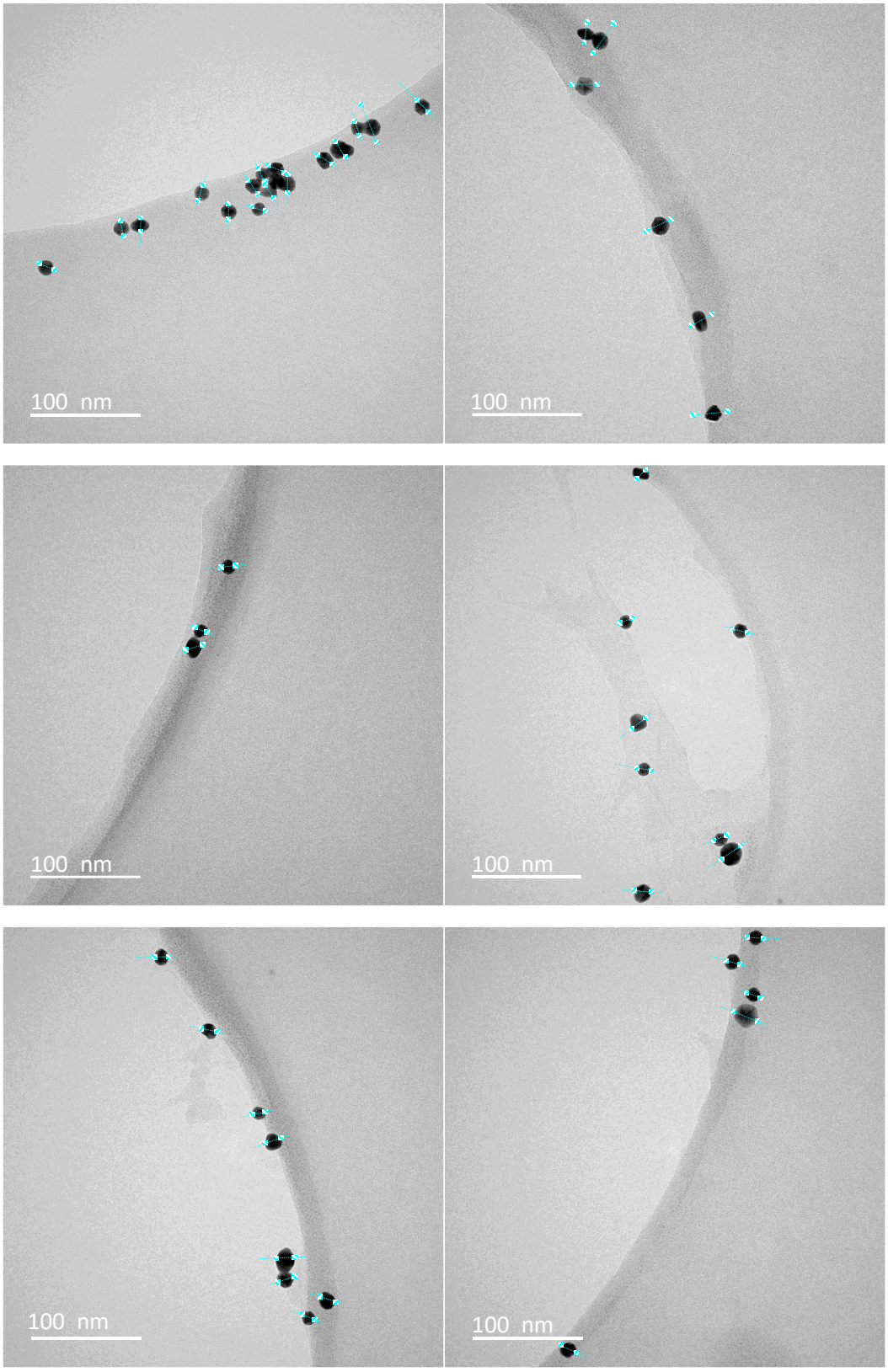

Figure S6. TEM images used to obtain the size distribution histogram shown Figure S4 (after reaction).

2.5 X-ray photoelectron spectroscopy (XPS)

XPS survey measurements of the AuNPs before and after catalysis confirm the presence of metallic gold in both samples, as indicated by the prominent Au 4d and Au 4f peaks (Figure S7 (A) and (B)). Both samples also show pronounced XPS peaks for carbon and oxygen, confirming the presence of organic capping agents (citrate) at the nanoparticle surfaces. Trace amounts of Na and Cl, also observed in the XPS survey spectra, indicate minor residues of sodium chloride (a by-product of the Au nanoparticle synthesis) in the samples.

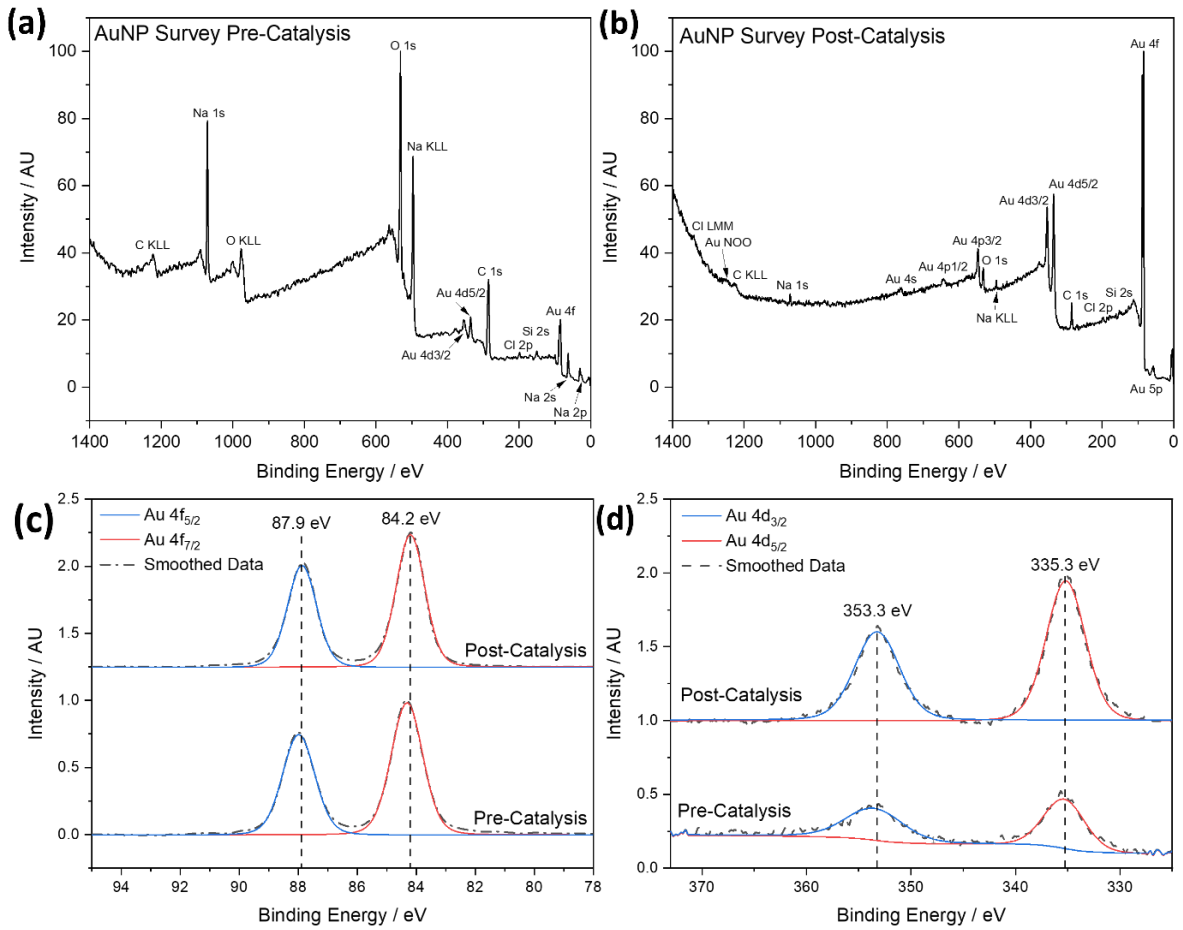

Figure S7. XPS spectra of AuNPs, (a) survey spectrum for AuNPs pre-catalysis, (b) survey spectrum for AuNPs post-catalysis, (c) high-resolution Au 4f spectra before and after catalysis, (d) high-resolution Au 4d spectra before and after catalysis.

The Au 4f high-resolution XPS spectra of both samples show the typical gold peaks at 84.2 eV and 87.9 eV, assignable to the Au $4f_{7/2}$ and Au $4f_{5/2}$ spin-orbit splitting, respectively (Figure S7 (C)). For both samples, the symmetric nature and the characteristic position of both peaks indicates that gold is only present in its metallic state. It is well-known that the gold $4f_{7/2}$ peak for Au(0) has a characteristic binding energy of 84.2 eV, as observed here for both samples.[3,4] Further, the presence of Au(I) and Au(III) can be excluded as this would give rise to clear distortion of the peak symmetries and large shifts in characteristic binding energy for the Au $4f_{7/2}$ peak to 85.6 eV and 86.5 eV, respectively.[5]

Comparing the high-resolution peaks of pre- and post-catalysis samples, no significant changes in peak position or peak symmetry are observed for the Au 4f and Au 4d high resolution spectra (Table 1). These XPS findings clearly indicate that no permanent change in Au oxidation was induced during the reaction, with the active nanoparticle surface atoms remaining in their metallic Au(0) state even after prolonged reaction times.

Table 1. Table showing the deconvoluted peak positions for the Au 4f and Au 4d high resolution XPS spectra before and after catalysis.

Peak	Peak Position / eV	
	Pre-catalysis	Post-catalysis
Au $4f_{7/2}$	84.3	84.2
Au $4f_{5/2}$	88.0	87.9
Au $4d_{5/2}$	335.3	335.2
Au $4d_{3/2}$	353.3	353.2

2.5.1 XPS sample preparation method

AuNPs were synthesised in batch using the method described in section 1.2.3. For the pre-catalyst sample, nanoparticles were directly sampled after synthesis. For the post-catalysis sample, nanoparticles were sampled after the catalytic reduction of nitrophenol (method described in section 6.1.), without further washing. For both samples, the original nanoparticle dispersions were concentrated via centrifugation-induced sedimentation (repeated centrifugation at 14,000 RPM for 5 min, with the supernatant from each run discarded and the tube refilled with more nanoparticle dispersion). The resulting concentrated AuNP dispersions were then drop-casted onto a silicon wafer and left to dry in air.

The spectra were obtained using a UHV-XPS system with a SPECS Phoibos 150 analyser with 1D-DLD detectors. The source was a monochromated Al anode (SPECS XR-50M) with an energy of 1486.7 eV. The energy resolution was estimated to be 0.2 eV at a pass energy of 30 eV for the high-resolution spectra and 1 eV (step size) at a pass energy of 30 eV for the survey spectra.

The data were processed using CasaXPS software. The spectra were calibrated against the adventitious C 1s peak, which was set to a binding energy of 284.8 eV. An intensity calibration was also applied using a transmission function file obtained from the instrument operator. The angular distribution correction was set to 54.7 °.

Survey spectrum quantification was performed using the quantify tool in CasaXPS. Shirley-type backgrounds were applied to the elemental peaks and subsequent integration of the peaks enabled quantification of the atomic surface concentrations. Default RSF values for each element were used to scale the peak areas. A Shirley background was also defined for the high-resolution spectra, which was then subtracted before peak fitting. No constraints on peak width or position were required due to the symmetric nature of the Au $4f_{7/2}$ and $4f_{5/2}$ peaks.

3 Equipment and Reactor setup

3.1 Equipment

Reactor. 7.1 m of 1/32" (ID) PTFE tubing (3.5 mL flow reactor).

Reagent pumps. Nitrophenol solution (0.6 mM): Jasco PU-980; pure water: Jasco PU-980; $NaBH_4$(aq) solution (10 mM): SyrDos2; and AuNP solution (0.167 mM): SyrDos1.

Reactor Unions. IDEX ETFE T-piece assemblies (part no. P-632).

Back Pressure Regulator. Spring based (40 psi) IDEX back pressure regulator (part no. P-761).

UV-vis spectrometer. FLAME-S-US-VIS OceanOptics (200-850 nm), DH-MINI deuterium tungsten halogen light source (200-2000 nm), QP400-2-SR-BX 400 um premium fibre optic cables and a CVF-Q-10 quartz flow cell (1 cm path length) in an OceanOptics CUV UV cuvette holder.

Software: The automation code (available on GitHub[6]) was written in MATLAB 2018a and the software ChemiView[7] was used record and monitor UV-vis spectra.

3.2 Reactor setup and configuration

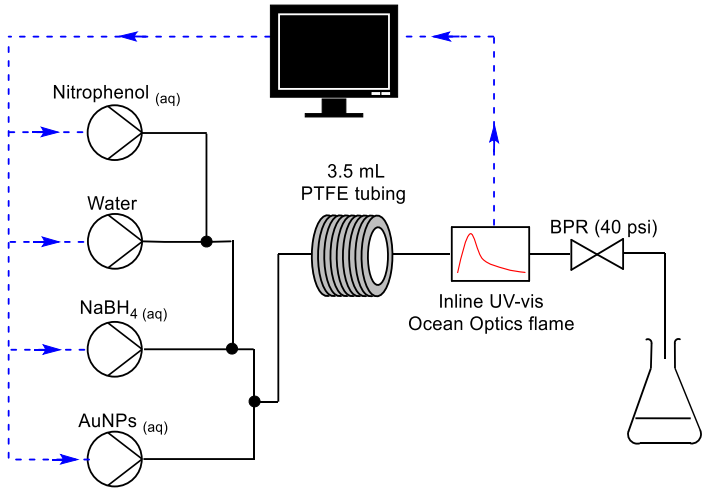

Figure S8. The above schematic shows an overview of the equipment used. Aqueous solutions of nitrophenol, $NaBH_4$ and AuNPs were pumped into a 3.5 mL PTFE tubular reactor and diluted to a desired concentration with a water pump, maintained at 40 psi pressure with a back-pressure regulator (BPR). The reactor was automated with code written in MATLAB, the reaction was monitored with an inline UV-vis spectrometer.

4 Reactor automation and data analysis

Method

Experimental conditions (see Table 1 in the manuscript) were suggested by the SNOBFIT algorithm and converted into the required pump. The time required for the reactor to reach steady state was calculated and then a timer started to trigger a UV-vis sample measurement once at steady state. UV-vis spectra were collected with ChemiView analysis software then deconvoluted via a process described in 5.1. The concentration of nitrophenol remaining in solution after the reaction was fed back to the SNOBFIT algorithm which then suggested the next set of experiments, if the maximum number of experiments had not yet been reached. To verify that no other products were formed during the reaction a AuNP catalysed nitrophenol reduction reaction was performed with $NaBH_4$ and analysed with HPLC, this confirmed complete conversion to the product 4-aminophenol and is in agreement with other studies of similar systems.[8,9] The automated optimisation process is described in Figure S9 below. Experimental conditions can be sent to the SNOBFIT algorithm in batches (e.g. batches of 4) in order of increasing temperature to reduce wait times when reactions when temperature is a factor, however, as all reactions were performed under constant temperature the snobfit code was run after each experiment to improve the efficiently of the optimisation algorithm.

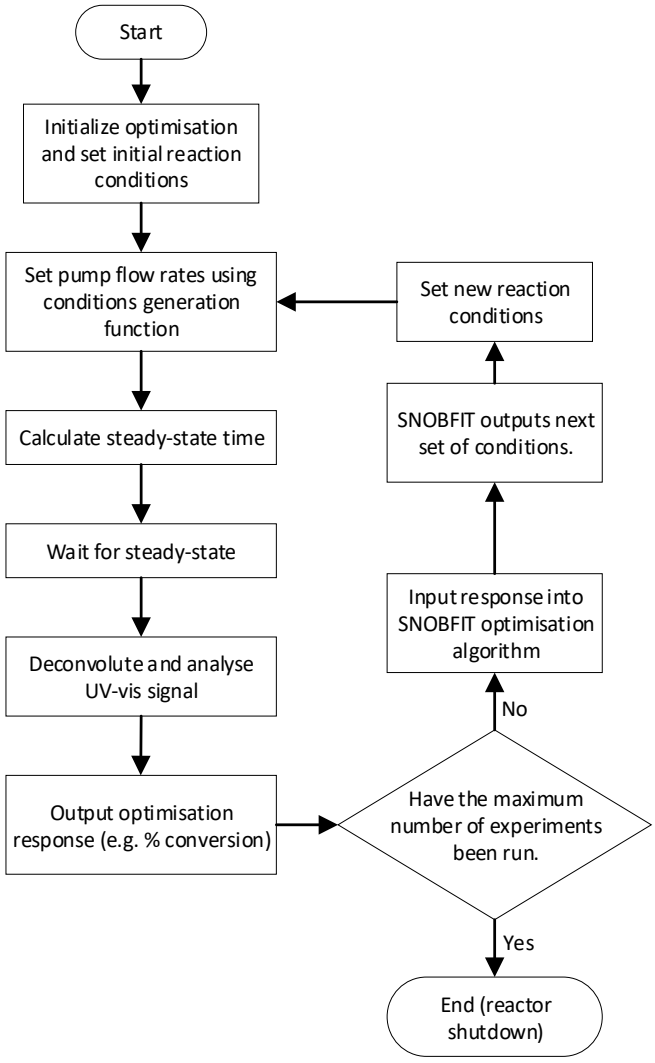

Figure S9. A flow diagram describing the automated processes by which the nanoparticle catalysed nitrophenol reduction reaction was optimised.

5 Calibration data

5.1 Spectral deconvolution

Inline UV-vis spectroscopy was used to determine the concentration of nitrophenol at the outlet of the reactor. A UV-vis calibration curve of was generated by integrated UV-vis absorption signal between 350-450 nm, for samples of pure nitrophenol at different concentrations (see section 5.2). However, due to the additive nature of UV—vis absorption spectroscopy, overlapping nitrophenol and AuNP (aq) spectra bands result in convoluted data (blue line, Figure S10). This systematic error was resolved using a deconvolution technique proposed by Sutherland, T.[10]

Nitrophenol (purple line, Figure S10) does not absorb light at wavelengths > 500 nm and AuNPs (aq) have a broad UV-vis absorption band which typically peaks between 500-560 nm. Therefore, it was possible to generate a prediction of the underlying AuNP abortion band by scaling an AuNP (aq) reference spectra to match the peak intensity in the measured spectrum between 500-560 nm (orange line, Figure S10). This predicted spectrum could then be subtracted from the overall absorption spectrum to obtain a prediction of how the absorption spectrum would appear without the AuNP (aq) absorption band (yellow line, Figure S10).

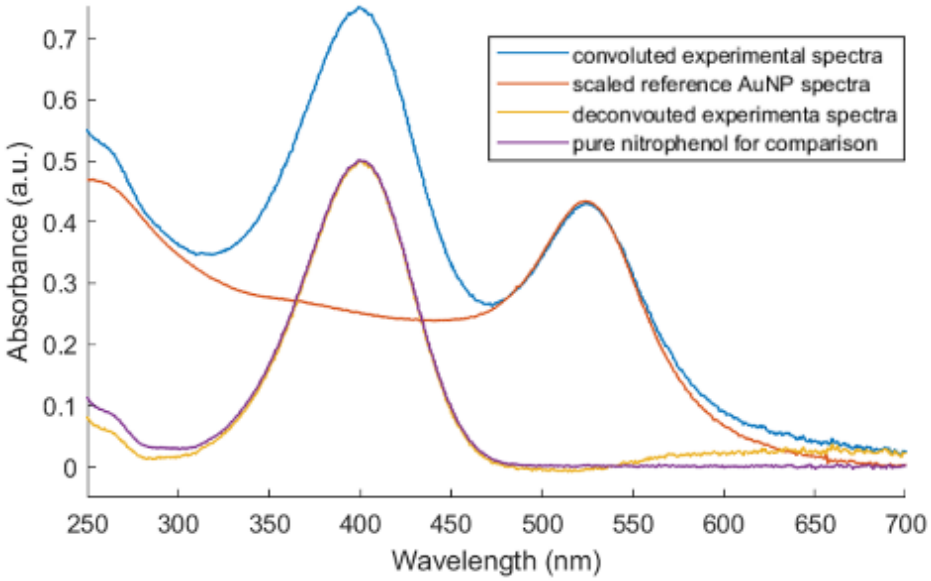

Figure S10. Plot showing an example of how the raw inline UV-vis signal from the optimisation was deconvoluted to obtain more accurate nitrophenol concentration measurements.

5.2 Nitrophenol calibration

Nitrophenol solutions with the following concentrations: 0.012, 0.024, 0.036, 0.048 and 0.06 mM were made to obtain the calibration gradient shown in Figure S12. Each calibration sample was injected into a to a CVF-Q-10 quartz flow cell (1 cm path length) in an OceanOptics CUV UV cuvette holder for UV-vis analysis. The UV-vis spectra were obtained using a FLAME-S-US-VIS OceanOptics spectrometer (200-850 nm) with a DH-MINI deuterium tungsten halogen light source (200-2000 nm) and QP400-2-SR-BX 400 um premium fibre optic cables.

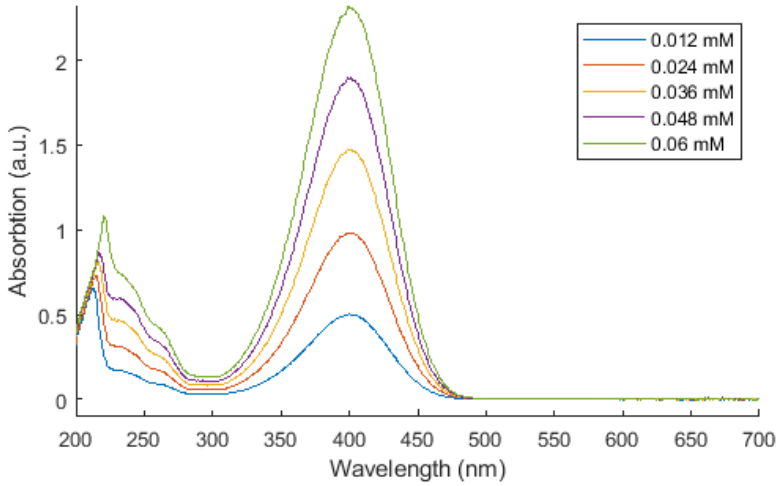

Figure S11. Plot showing absobtion bands for 5 nitrophenol calibration standards from 0.012 to 0.06 mM.

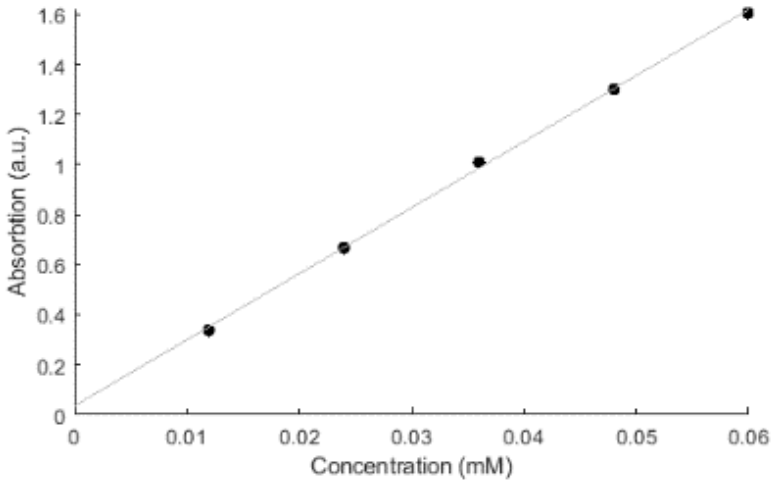

Figure S12. A calibration plot showing the intergrated absorbtion values for nitrophenol calibration standards (adjusted to pH 10), between 350 - 450 nm, for 5 nitrophenol calibtation standards from 0.012 to 0.06 mM. Gradient 26.439, Intercept 0.03344, R-squared value: 0.999.

6 Kinetic modelling and batch validation reaction

As a high data density was achieved as a result the self-optimisation study, this data could be fitted to a physical model of our chemical system with a genetic algorithm. The Langmuir-Hinshelwood model was employed, as this is a commonly accepted kinetic model for bi-molecular surface catalysed reactions (eq. 2). Where k is the rate constant for the reaction, S is the AuNP surface area (see section 2.2), C_{Nit}/C_{BH_4} are the concentrations of nitrophenol/ sodium borohydride and K_{Nit}/K_{BH_4} are the absorption coefficients of nitrophenol/sodium borohydride.

$$v = \frac{dC_{Nit}}{dt} = \frac{K_{Nit}C_{Nit}K_{BH_4}C_{BH_4}}{\left(1 + K_{Nit}C_{Nit} + K_{BH_4}C_{BH_4}\right)^2} kS \quad (2)$$

Ordinary differential equation (ODE) solvers were used to predict how the reaction would proceed when different model co-efficients were applied. To build a model based on the results of the optimisation, a genetic algorithm[11] was used to maximise the convergence of simulated and experimental reaction conversions by minimising the sum of squared error (SSE) metric (eq. 3). Where: E_x and S_x are the experimental and simulated data points of time x, and n are the total number of data points, similar to the approach used by the kinetic fitting software Compunetics.[12] As each data point has a differing gold nanoparticle surface area and residence time, each isolated point is fitted using their respective initial conditions subject to the changing values of k, K_{Nit} and K_{BH_4}.

$$SSE = \sum_{x=1,2,3,\ldots,n} (E_x - S_x)^2 \quad (3)$$

After the fitting converged on kinetic parameters for the data set, Monte Carlo simulations were performed to assess the robustness of the fitting and to identify the error in both the experimental and fitting aspects of the methodology. The relative error in the analytic equipment was found to be 0.5 %, therefore 100 Monte Carlo simulations were performed with a random ± 0.5 % relative error added to all experimental data. After all kinetic fitting was conducted, the convergence of the simulated reactions to the real experimental data was very high, with an average residual error of only 1.66 %.

Table 2. The kinetic parameters identified from kinetic fitting.

k /M^{-1} m^2 s^{-1}	2.46 ± 0.05
K_{Nit}	1.47 ± 0.02
K_{BH_4}	12.17 ± 0.2

6.1 Batch validation experiment

To validate the kinetic model, a batch reaction was performed as follows. AuNPs (24 mL, synthesised using the method described in section 1.2.3) were added to a 50 mL stirred solution of 0.24 mM nitrophenol in a 250 mL round bottomed flask, an additional 20 mL of water was added to make the solution up to 94 mL. The reaction was initiated by adding 6 mL of a freshly made 28 mM sodium borohydride solution bringing the final total volume to 100 mL. The reaction mixture was stirred and recirculated through a short length of tubing with a peristaltic pump to a UV-vis flow cell for continuous monitoring, the reactor setup is shown in Figure S13.

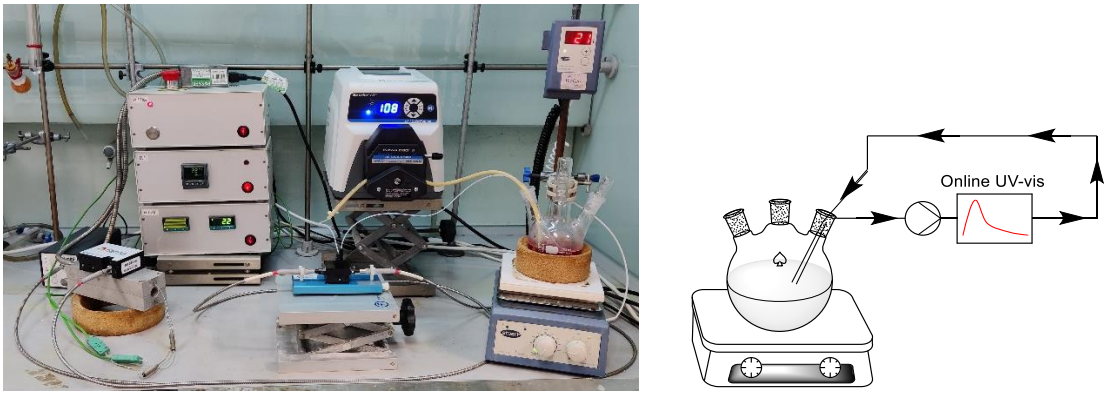

Figure S13. A 250 mL round bottomed flask containing a 100 mL stirred reaction solution was recirculated through a UV-vis flow cell for continuous monitoring.

7 Data from Optimisation

Table 3. Table showing experiments performed during the optimisation, this data corresponds to Fig 2 in the manuscript.

Experiment Number.	$NaBH_4$ conc. (mM)	Gold NP SA. ($m^2 L^{-1}$)	Residence time (min)	Conversion (%)
1	2.1294	0.06	2.2886	45.76
2	0.65	0.05	1.2	20.696
3	0.85	0.05	2.8	25.102
4	2	0.08	1.1	28.227
5	1.2	0.15	1.9	73.601
6	1.8	0.11	3	83.502
7	1.3	0.14	1.1	47.172
8	0.55	0.11	2.2	50.738
9	1.85	0.10	1.7	48.704
10	0.95	0.14	2.6	62.12
11	1.75	0.16	3	94.777
12	0.55	0.16	1.1	64.729
13	0.95	0.10	2.6	39.136
14	1.75	0.07	2.65	47.423
15	2.5	0.16	3	93.226
16	1.7	0.12	1.4	45.078
17	2.1	0.16	3	95.04
18	1	0.08	1.6	22.034
19	2.5	0.12	3	80.44
20	1.6	0.10	2.65	60.148
21	2	0.16	3	92.12
22	0.85	0.13	1.7	47.926
23	2.15	0.08	2.4	48.769
24	0.75	0.15	2.3	58.761
25	2.35	0.09	2.75	58.067
26	1.9	0.12	2.5	68.625
27	2.4	0.09	2.45	57.014
28	2.15	0.13	2.05	67.3722
29	2.5	0.16	2.5	87.2598

8 References

1. Bastus, N. G. *et al.* Kinetically Controlled Seeded Growth Synthesis of Citrate-Stabilized Gold Nanoparticles of up to 200 nm: Size Focusing versus Ostwald Ripening. *Langmuir* **27**, 11098–11105 (2011).

2. Spreadborough, J. & Christian, J. W. High-temperature X-ray diffractometer. *J. Sci. Instrum.* **36**, 116–118 (1959).

3. Radnik, J., Mohr, C. & Claus, P. On the origin of binding energy shifts of core levels of supported gold nanoparticles and dependence of pretreatment and material synthesis. *Phys. Chem. Chem. Phys.* **5**, 172–177 (2003).

4. Tchaplyguine, M., Mikkelä, M. H., Zhang, C., Andersson, T. & Björneholm, O. Gold oxide nanoparticles with variable gold oxidation state. *J. Phys. Chem. C* **119**, 8937–8943 (2015).

5. Casaletto, M. P., Longo, A., Martorana, A., Prestianni, A. & Venezia, A. M. XPS study of supported gold catalysts: the role of Au0 and Au+δ species as active sites. *Surf. Interface Anal.* **38**, 215–218 (2006).

6. Hall B. https://github.com/blhall195/Automated_nanoparticle_reaction_optimisation

7. Avila C. ChemiView V3.4. http://chemiview.leeds.ac.uk.

8. Aditya, T., Pal, A. & Pal, T. Nitroarene reduction: A trusted model reaction to test nanoparticle catalysts. *Chemical Communications* vol. 51 9410–9431 (2015).

9. Hervés, P. *et al.* Catalysis by metallic nanoparticles in aqueous solution: Model reactions. *Chem. Soc. Rev.* **41**, 5577–5587 (2012).

10. Sutherland, T. I. *et al.* Effect of ferrous ion concentration on the kinetics of radiation-induced iron-oxide nanoparticle formation and growth. *Phys. Chem. Chem. Phys* **19**, 695–708 (2017).

11. Goldberg, D. E. *Genetic Algorithms in Search, Optimization and Machine Learning*. (Addison-Wesley Longman Publishing Co., Inc., 1989). doi:10.5555/534133.

12. Taylor, C. J. Compunetics. (2020).